CHEMMEDCHEM

CHEMISTRY ENABLING DRUG DISCOVERY

Accepted Article

Title: Form Matters: Stable Helix Foldamers Preferentially Target Human Monocytes and Granulocytes

Authors: Claudia Tomasini, Nicola Zanna, Lorenzo Milli, Benedetta Del Secco, Andrea Cornia, Regina Tavano, Emanuele Papini, and Giulia Malachin

To be cited as: *ChemMedChem* 10.1002/cmdc.201600597

Link to VoR: http://dx.doi.org/10.1002/cmdc.201600597

A Journal of

ChemPubSoc Europe

WILEY-VCH

www.chemmedchem.org

Form Matters: Stable Helical Foldamers Preferentially Target Human Monocytes and Granulocytes

Benedetta Del Secco,[a] Giulia Malachin,[b] Lorenzo Milli,[a] Nicola Zanna,[a] Emanuele Papini,[b] Andrea Cornia,*[c] Regina Tavano,*[b] Claudia Tomasini* [a]

Abstract: Some hybrid foldamers of different length all containing the D-Oxd moiety alternated with a L-amino acid (L-Val, L-Lys or L-Ala) have been prepared to study their preferred conformations and to evaluate their biological activity. Surprisingly, only the longer oligomers containing L-Ala fold into well-established helices, while all the other oligomers give partially unfolded turn structures. Nevertheless, they all show a good biocompatibility, with no detrimental effects up to 64 μM concentration. After equipping some selected foldamers with the fluorescent tag Rhodamine B, a quantitative analysis was obtained by dose and time response analysis by FACS of human HeLa cells, and primary blood lymphocytes, granulocytes and monocytes. Among the analyzed cell types, these oligomers associated with monocytes and granulocytes with best efficacy, still visible after 24 h incubation. This effect is even more pronounced for foldamers able to form stable helices.

Introduction

The understanding of sophisticated interplays between structure and function of molecules within complex systems is a great challenge in life sciences. Selective labeling of biomolecules with bio-physical probes in principle allows for investigation and manipulation of proteins, enzymes or biochemical processes in vitro as well as in vivo.[1] Various biological and biophysical methods may be used to study the internalization mechanism, to localize and to quantify the peptides internalization together with their cargoes inside cells. Yet, any method has its pitfalls, so a combination of different approaches is often needed to have access to the large pictures.

The fluorescence-based protocol requires the preparation of a peptide that is covalently coupled to a fluorophore. Its measurement by fluorescence (fluorimetry) enables the peptide indirect quantification and confocal microscopy allows its localization inside living cells.

Rhodamine dyes are well known synthetic molecules used for fabrics dyeing and belong to the class of xanthene dyes.[2] These fluorescent markers are used as fluorescent probes in biological studies, in structural microscopic studies, photosensitizers and laser dyes. They may be successfully introduced in synthetic structures,[3] called “foldamers”.[4,5] This neologism refers mainly to medium-sized molecules (about 500–5000 Dalton) that fold into definite secondary structures (i.e., helices, turns and sheets), thus being able to mimic biomacromolecules despite their smaller size. Applications [6,7] have ranged from cellular penetration [8] and membrane disruption to discrete molecular recognition.[9,10] Hybrid foldamers, containing the (4*R*,5*S*)-4-carboxy-5-methyl-oxazolidin-2-one (D-Oxd) unit alternated with an α- or β-amino acid, have been extensively studied by our research group,[11] as the D-Oxd moieties impart rigidity to the peptide chain,[12–14] while the L-amino acids promote the folding.[15–17]

In the past, the Gellman group suggested that the formation of a globally amphiphilic helix is not required for host-defense peptide mimicry,[18] as also amphiphilic conformations of random copolymers without any helical structure were proven to exhibit potent antibiotic activity. Other studies [19,20] demonstrated that only the *Aib*-based foldamers forming a precise helical-spherical domain can target human monocytes, macrophages and dendritic cells more effectively than non-immune cells. In this work we describe some hybrid foldamers of different length all containing the D-Oxd moiety alternated with a L-amino acid (L-Val, L-Lys or L-Ala), to check any possible relationship between their preferred conformations and their behavior towards leukocytes.

The foldamers were functionalized with Rhodamine B (RB) (Figure 1) in order to measure their interactions with cells by fluorescence techniques.[21] For an efficient synthesis of all the conjugates, we developed a cheap and straightforward protocol to introduce RB in a polypeptide chain, based on a microwave-assisted reaction.

[a] B. Del Secco, Dr. L. Milli, Dr. N. Zanna, Prof. C. Tomasini
Dipartimento di Chimica Ciamician
Alma Mater Studiorum Università di Bologna
Via Selmi 2, 40126 Bologna (Italy)
E-mail: claudia.tomasini@unibo.it
[b] Dr. G. Malachin, Prof. E. Papini, Dr. R. Tavano
Dipartimento di Scienze Biomediche
Università di Padova
Viale G. Colombo 3, 35121 Padova (Italy)
E-mail: regina.tavano@unipd.it
[c] Prof. A. Cornia
Dipartimento di Scienze Chimiche e Geologiche
Università di Modena e Reggio Emilia & INSTM
Via G. Campi 103, 41125 Modena (Italy)
E-mail: acornia@unimore.it

Supporting information for this article is given via a link at the end of the document.

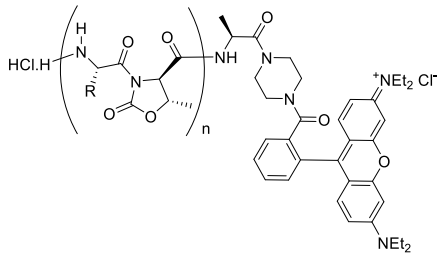

Figure 1. General structure of the foldamers described in this work.

Results and Discussion

D-Oxd-OBn was obtained in high yield starting from D-Thr in multigram scale,[17] and coupled with *N*-protected L-Val or L-Lys in the presence of HBTU [*O*-(benzotriazol-1-yl)-*N,N,N′,N′*-tetramethyluronium hexafluorophosphate] and DIEA (di-isopropyl ethyl amine) to prepare **1** and **2** that were used to access complex foldamers (for all the synthetic details, see SI) (Scheme 1). These amino acids have been chosen as they have very different polarity, being L-Val a lipophilic amino acid, while L-Lys is a basic and hydrophilic amino acid. Additionally, they have been extensively used in the past for the preparation of bioactive peptides.[18,22,23]

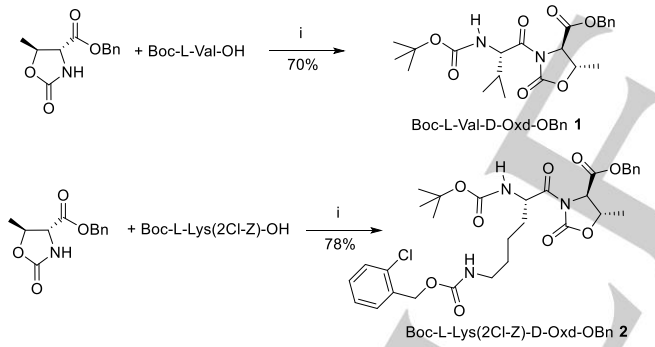

Scheme 1. Reagents and Conditions: (i) HBTU (1.1 equiv.), DIEA (2 equiv.), dry CH_3CN, 1 h, r.t.

Compound **2** was prepared using Boc-L-Lys(2Cl-Z)-OH, as the 2Cl-Z group is stable towards hydrogenolysis under mild conditions (Scheme 1). Complex foldamers **3**, **5** and **7** and the corresponding fully deprotected oligomers **4**, **6** and **8** have been prepared in solution alternating the two moieties (Scheme 2). For the biological essays, trifluoracetate counterions should be avoided, so the deprotection of compounds **4**, **6** and **8** with trifluoroacetic acid was replaced with a protocol envisaging hydrochloric acid,[24] that afforded fully deprotected oligomers as hydrochloride salts in high yield.

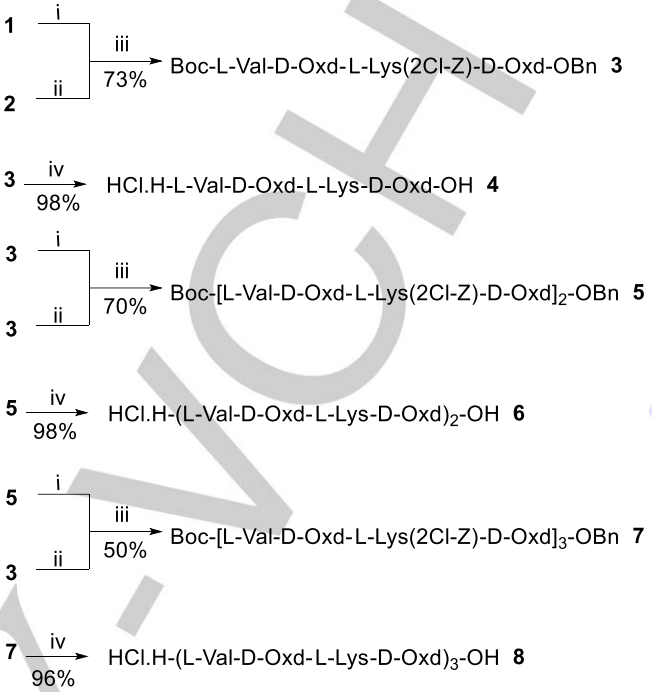

Scheme 2. Reagents and Conditions: (i) H_2, Pd/C (10%), MeOH, r.t., 16 h; (ii) TFA (18 equiv.), dry CH_2Cl_2, r.t., 4 h; (iii) HBTU (1.1 equiv.), DIEA (2 equiv.), dry CH_3CN, 1 h, r.t.; (iv) Pd/C (10%), 11 M HCl, dry MeOH, 4 h, r.t; then 2,2,2-trifluoroethanol, dry CH_2Cl_2, 3 h, r.t.

Using the same deprotection technique, we synthesized the foldamers HCl.H-(L-Ala-D-Oxd)$_n$-OH (n = 2, 4, 6) **9**, **10** and **11**, starting from the already reported foldamers Boc-(L-Ala-D-Oxd)$_n$-OBn.[15]

The biocompatibility of fully deprotected oligomers of both series was checked. HeLa cells were seeded and incubated for 24h with compounds **4**, **6**, **8**, **9**, **10** and **11** at different concentrations, then cells were washed, MTS solution was added and the absorbances were read by an ELISA reader after 30 minute incubation. All tested oligomers have demonstrated to be non-toxic up to 64 µM concentration and after a 24 hours incubation to HeLa cells, irrespective of length and charge (Figure 2). This outcome suggests a good biocompatibility of our foldamers formulations.

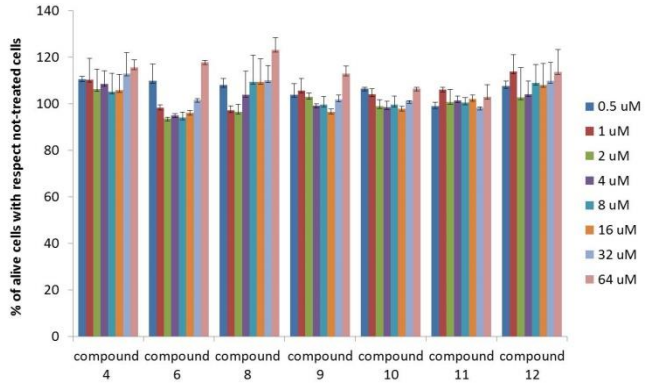

Figure 2. MTS assay performed on the fully deprotected foldamers HCl.H-(L-Val-D-Oxd-L-Lys-D-Oxd)$_n$-OH **4**, **6** and **8** and HCl.H-(L-Ala-D-Oxd)$_n$-OH **9**, **10** and **11**. Percentages of alive cells were obtained with respect to non-treated cells. Results are representative of one experiment run in triplicate.

Synthesis and Biological Evaluation of the Rhodamine B Containing Oligomers

To gain a deeper insight into the influence of the foldamer nature on cellular uptake, foldamers **4**, **8**, **9** and **11** have been coupled with a fluorescent moiety. They differ for chain length (**4** and **9** are short, while **8** and **11** are long oligomers) and for the amino acid choice, as **4** and **8** contain L-Val and L-Lys, while **9** and **11** contain only L-Ala. To avoid the use of expensive fluorescein isothiocyanate,[25] we developed a new method to couple our foldamers with the cheap RB.

By modification of a well-known procedure,[26,27] we added RB base **12** to piperazine-trimethyl aluminium in toluene (Scheme 3). The reaction mixture was stirred under microwave irradiation at 50 W for 1 h, then acidified, filtered and purified by crystallization. The resulting derivative piperazine-Rhodamine B (P-RB) **13** was obtained in excellent yield and was then coupled with Boc-L-Ala-OH in the presence of HATU [1-[Bis(dimethylamino)methylene]-1*H*-1,2,3-triazolo[4,5-*b*]pyridinium 3-oxide hexafluorophosphate] and DIEA in high yield to afford pure Boc-L-Ala-P-RB **14** after flash chromatography. The labelled derivatives **16**, **18**, **20** and **22** have been obtained by standard coupling reaction in solution with satisfactory overall yields (Scheme 4).

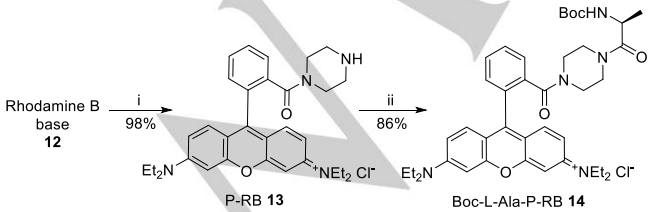

Scheme 3. Reagents and Conditions: (i) $AlMe_3$ (2 equiv.), piperazine (4 equiv.), toluene, MW 50W, 1h; (ii) Boc-L-Ala-OH (1 equiv.), HATU (1.1 equiv.), DIEA (2 equiv.), dry acetonitrile, 1 h, r.t.

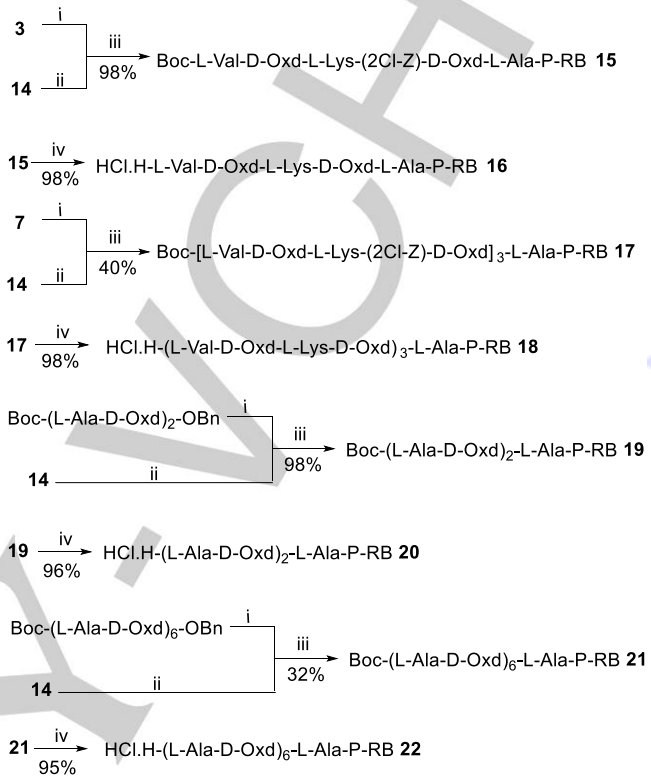

Scheme 4. Reagents and Conditions: (i) H_2, Pd/C (10%), AcOEt, r.t., 2 h ; (ii) TFA (18 equiv.), dry CH_2Cl_2, r.t., 4 h; (iii) HATU (1.1 equiv.), DIEA (3 equiv.), dry CH_3CN, 1 h, r.t.; (iv) H_2, Pd/C (10%), 12M HCl (4 equiv.), AcOEt, r.t., 2 h.

Initially we performed a qualitative analysis of the ability of our foldamers to target human monocytes purified from buffy coats using confocal microscopy. Data indicated that all the analyzed Rhodamine-labelled analogues are readily captured by monocytes, and that the best result is obtained with **22** (Figures 3 and S1). The cytosolic distribution of the fluorescence signal of labelled analogues is punctuated and clearly reminiscent of an endocytic mechanism of cell accumulation in monocytes. Similar experiments with granulocytes did not give interpretable intracellular distribution information, because of the small dimension and high background of these cells, while the signal from lymphocytes and HeLa cells was not strong enough.

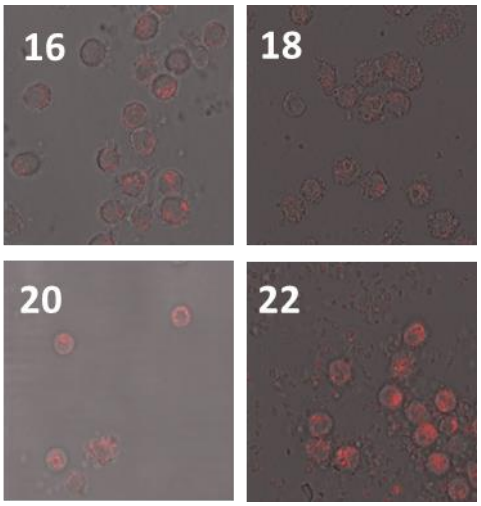

Figure 3. Confocal analysis of human monocytes after purification from buffy coats of healthy donors, seeding and incubation for 18h (20 µM) with foldamers **16**, **18**, **20** and **22**. The cells were washed with PBS and directly analyzed by confocal microscopy.

Therefore, to overcome these problems, a study was carried out by a dose and time response analysis by more sensitive and quantitative Fluorescence Activated Cell Sorting (FACS) approach. Purified human lymphocytes, granulocytes, monocytes and HeLa cells were incubated for 3 or 24 hours at 37°C with foldamers **16**, **18**, **20** and **22**, and with H-L-Ala-P-RB for comparison (Table 1). The cells were then washed with PBS, recovered and directly analyzed by cytofluorimetry.

In the case of the L-Ala series, **22** shows the best cell association especially after a 3 h incubation, while **20** capture was not distinguishable from the background, estimated by the cell association of H-L-Ala-P-RB, at any time. Moreover inflammatory monocytes and granulocytes are targeted by **22** more effectively than HeLa cells and lymphocytes even after 24 h incubation. Such effect was strongly inhibited by decreasing the incubation temperature to 0°C, a condition blocking active endocytosis of foldamers and only permitting their binding to cells (Figure S2). Collectively, data indicate that **22** is taken up by cells better than shorter **20** analogue and can preferentially target blood myeloid cells (monocytes and granulocytes) than lymphoid and epithelial cells. Such selectivity is peculiar and is reminiscent of observed in the same conditions, with the peptidic part of Trichogin, a well-known foldamer with a stable α-helix structure.[20]

Since cells have a negative superficial charge, the multiple cationic sites in foldamers **16** and **18** should in principle favor cellular association. As could be foreseen, the cell association of the short **16** oligomer is increased compared to **20**, although with a slow kinetics, being the improvement better visible after 24 h than after 3 h. In contrast, the introduction of three additional positive charges in foldamer **18** decreases its cell capture efficacy compared to **22**, and this effect is marked after short incubation time. Although **16** and **18** displayed the same cell selectivity, the kinetics of cell association was slower than for **22**.

Moreover, comparing the capacity of oligomers with different length to accumulate in different cell types provides interesting results, as the oligomers length strongly modulates the capture by any cellular model. While short oligomers weakly interact with cells, **22** shows a clearly improved cell-association capacity already after 3 h incubation.

Finally, among the analysed cells types, monocytes and granulocytes captured all the oligomers with best efficacy (6-7 times more effectively than HeLa and lymphocytes). Such a sustained cell capture is still visible after 24 h incubation.

To explain the good results obtained with **22**, we performed the conformational analysis of our foldamer series, including **4**, **8**, **9** and **11**. As described in the next section, we indeed found that a distinctive feature of the long L-Ala-D-Oxd oligomer **11** is its tendency to fold into stable helices.

Conformational Analysis

To check the presence of intramolecular N-H•••O=C hydrogen bonds in the fully protected oligomers **3**, **5** and **7**, IR and ^{1}H NMR spectra were recorded in the structure supporting solvents CH_2Cl_2 and $CDCl_3$, respectively. From IR analysis, all studied foldamers feature free N-H amide groups in CH_2Cl_2 solution.[28] However, when moving from **3** to **7**, the amount of intramolecular N-H•••O=C hydrogen bonds increases as shown by a broad band centered at about 3250 cm^{-1} (for a more detailed discussion, see SI and Figure S3).

A confirmation of these results was obtained by investigating the DMSO-d_6 dependence of NH proton chemical shifts in NMR spectra.[29] Compounds **3** and **5** give large $\Delta\delta$ values of about 1 ppm, suggesting that their NH hydrogens are not involved in intramolecular H-bonding. By contrast, the five NH groups of longer foldamer **7** are less sensitive to DMSO-d_6 addition and display moderately to strongly reduced $\Delta\delta$ values (0.77 to 0.33 ppm) (Table S1 and Figure S4).

In contrast, the conformational analysis of the fully protected foldamers Boc-(L-Ala-D-Oxd)$_n$-OBn has been previously reported.[15] We unambiguously proved that the oligomers having general formula Boc-(L-Ala-D-Oxd)$_n$-OR (n = 1-6, R = Bn or H) fold into ordered structures when n ≥ 5. From CD spectra we could demonstrate that the secondary structure adopted is a β-bend ribbon spiral, which is a subtype of the 3_{10}-helix.

Then, we also relied on ECD spectroscopy to directly investigate the conformation adopted by our new foldamers series in water solution. Since the Rhodamine dye is a strong fluorophore and inhibits the ECD analysis, we registered the ECD spectra of the unlabelled foldamers **4**, **8**, **9** and **11** (Figure 4). In the labelled compounds the Rhodamine moiety is connected to one end of the chain and should not affect the preferred foldamer conformation.

Table 1. Association of foldamers **16**, **18**, **20**, **22** and of H-L-Ala-P-RB to different human cells after 3 hours incubation (left) and after 24 hours incubation (right). Results are representative of one experiment run in duplicate. MFI: mean fluorescence intensity.

Foldamer	After 3 hours	After 24 hours
16	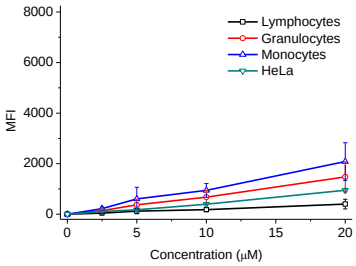	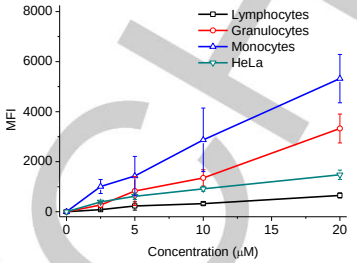
18	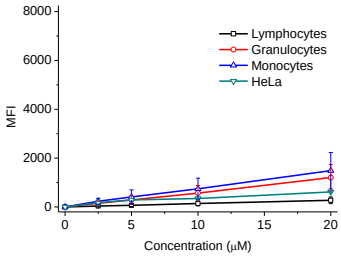	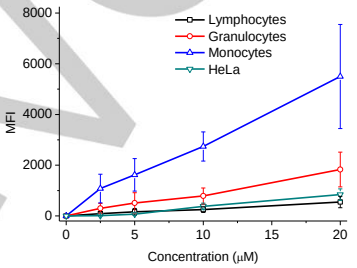
20	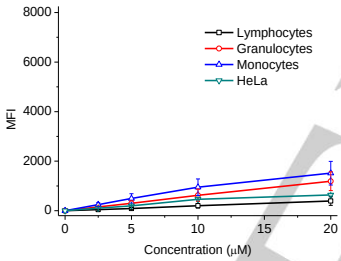	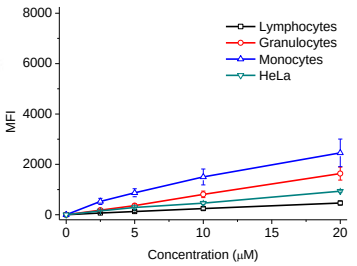
22	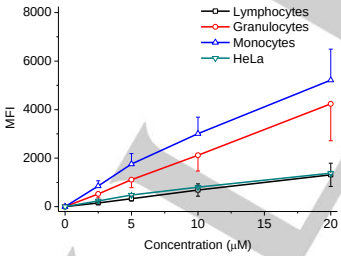	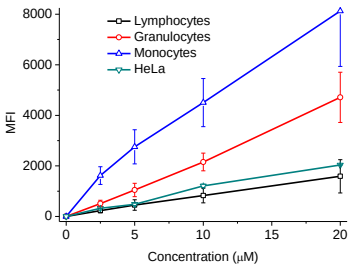
H-L-Ala-P-RB	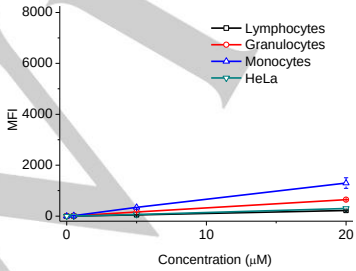	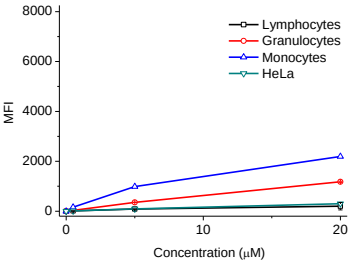

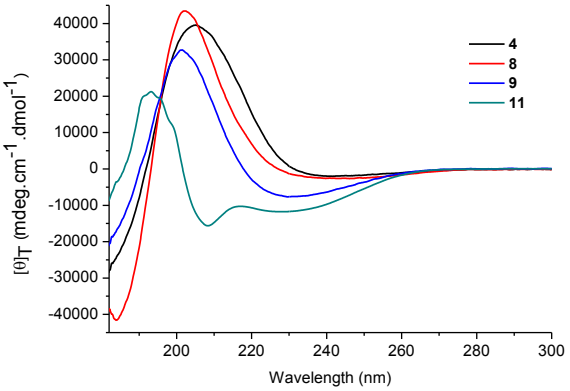

Figure 4. Normalized *per*-residue ECD spectra of compounds **4**, **8**, **9** and **11** in H_2O solution (3 mM, room temperature).

The *per*-residue ECD spectra of foldamers **4**, **8** and **9** are very similar as they all display a strong negative signal at 182-185 nm and a positive band at 202-204 nm. Foldamers **4** and **8** also exhibit a broad and weak negative band centered at 240 nm, while **9** shows a more intense broad negative band centered at 230 nm. The modest variations across the three spectra suggest that these oligomers do not assume a helical conformation but rather fold in a turn conformation.[30] Unlike the α-helix and β-sheet, there is no unique ECD signature for turns because of the range of conformers included in this structural category.[31] Various spectral patterns were predicted, but the predominant one had a weak negative $n \rightarrow \pi*$ band at 220–230 nm and two strong $\pi \rightarrow \pi*$ bands, a positive one at 200–210 nm and a negative one at 180–190 nm.[32]

In contrast, the spectrum of **11** displays a strong positive signal at 193 nm and two negative bands centered at 208 and 228 nm respectively, with $R = [\theta]_{228}/[\theta]_{208} = 0.75$, like the parent Boc-(L-Ala-D-Oxd)$_6$-OH compound.[15] This is the typical ECD signature of 3_{10} helices, in agreement with the work of Toniolo and coworkers [33,34] and with theoretical calculations.[35] Both experimental and theoretical studies point to the following main characteristics of the 3_{10}-helix: (a) a negative ECD band centred near 207 nm; (b) a negative shoulder in the vicinity of 222 nm; (c) a $R = [\theta]_{222}/[\theta]_{207}$ ratio smaller than reported for the α-helical peptides, where R is usually close to 1; (d) a positive maximum al 198 nm.

Foldamers **8** and **11** have the same number of residues and should adopt the same preferred conformation. The unexpected turn structure in **8** may be attributed to the presence of sterically demanding residues and of residues which can form side-chain to main-chain intra-strand H-bonds.

To probe the conformation of these materials in the solid state, we tried to crystallize foldamers of the two series in both protected and deprotected forms. Since it is known that crystallization is more difficult for enantiomerically pure chiral molecules than for the corresponding racemates,[36–39] we also synthesized enantiomers and prepared racemates. It is still not clear whether more facile crystallization of racemic protein mixtures is a general phenomenon,[40] but racemic crystallization has been extensively studied for proteins, short peptides[41] and DNA.[42] Recently, this technique and X-ray crystallography have been successfully applied to the determination of the unknown structure of snow flea antifreeze protein (sfAFP),[43] and of the crystal structures of seven tripeptides in enantiomeric and racemic forms.[44]

After several attempts, X-ray quality crystals of *rac*-Boc-L-Ala-D-Oxd-OBn, Boc-(D-Ala-L-Oxd)$_2$-OBn and Boc-L-Val-D-Oxd-L-Lys(2Cl-Z)-D-Oxd-OBn (**3**) were grown by slow evaporation of ethyl acetate or chloroform solutions. Crystals of Boc-(D-Ala-L-Oxd)$_2$-OBn were obtained from the racemate and spontaneous resolution thus occurred during crystallization (see Experimental Section for details on absolute structure determination). Unfortunately, we were not able to grow suitable crystals of the longer foldamers. The molecular structures of Boc-L-Ala-D-Oxd-OBn, Boc-(L-Ala-D-Oxd)$_2$-OBn and **3** are depicted in Figures 5 and 6 (for an easier comparison, we show enantiomers with the same absolute configuration at corresponding chiral centers). Additional plots of molecular and crystal structures are provided as Figures S6-S11. All crystal data and refinement parameters are given in Table S2 while the geometry of hydrogen-bond interactions and conformational data are gathered in Tables S3-S5 and S6-S8, respectively.

In the solid state, the three compounds do not form *intra*molecular N-H•••O=C hydrogen bonds. Amide nitrogen atoms are involved only in *inter*molecular hydrogen bonds or in no H interaction at all, like for the amide nitrogen N1 in Boc-(D-Ala-L-Oxd)$_2$-OBn. The emerging picture thus agrees well with solution ECD data (see above and Ref. [15]). Secondary structure relies just on C-H···O interactions: in the three studied foldamers, the α-carbon atom of each amino acid residue has an H contact with the endocyclic carbonyl oxygen of the neighboring Oxd moiety (see captions to Figures 5 and 6 for details). Such a nonclassical hydrogen bond is commonplace in the solid state structure of Oxd-based foldamers[11,15,45,47] and persists in solution, as judged by the chemical shift of α-protons in NMR spectra.[14,15,17,47]

Turning now to intermolecular interactions in the solid state, *rac*-Boc-L-Ala-D-Oxd-OBn entails centrosymmetric supramolecular dimers held together by a pair of N-H•••O=C bonds between the two antiparallel peptide segments. In Boc-(D-Ala-L-Oxd)$_2$-OBn and **3**, a classical H-bond is formed between the amide nitrogen N3 and carbonyl oxygen O2 of the same peptide segment, but belonging to a neighboring, antiparallel molecule in the crystal. A similar chain-like supramolecular arrangement based on a single classical H bond was previously found in Boc-(L-Phe-D-Oxd)$_n$-OBn, the alignment of peptide units being parallel and antiparallel for n = 1 and 2, respectively.[48,49]

Figures 5 and 6 and inspection of backbone torsion angles (Tables S6-S8) indeed show that the three compounds adopt similar, partially extended conformations, in agreement with ECD studies. Conformational parameters at L-Ala residues (ϕ = -87.4 ÷ -70.3°, ψ = 147.4 ÷ 173.4°) correspond approximately to those characteristic of PPII structure,[50] while the conformation at the L-Val and L-Lys residues in **3** (ϕ = -134.3 ÷ -132.2°, ψ = 150.6 ÷ 172.0°) is more reminiscent of peptide β strands.[51]

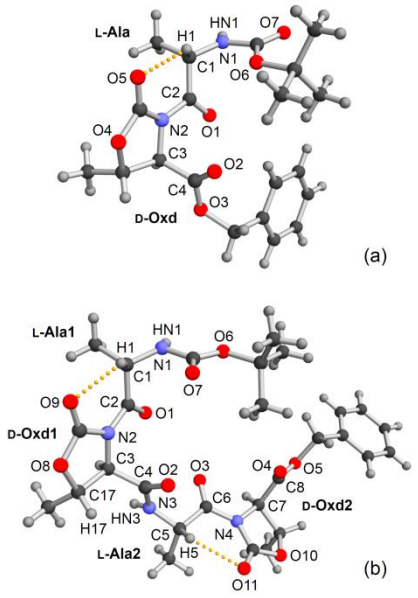

Figure 5. Molecular structure of (a) Boc-L-Ala-D-Oxd-OBn molecule in *rac*-Boc-L-Ala-D-Oxd-OBn and of (b) Boc-(L-Ala-D-Oxd)$_2$-OBn, obtained by inversion of the experimental model. Atoms are drawn as spheres with arbitrary radius. Labels are provided for all N and O atoms, for backbone carbons as well as for C and H atoms relevant to H bonding. Color code: C = dark grey, N = blue, O = red, H = light grey. Intramolecular nonclassical H bonds are represented as yellow dotted lines. Selected interatomic distances (Å) and angles (°): in (a), H1···O5 = 2.290(13), C1-H1···O5 = 121.2(10); in (b), H1···O9 = 2.27, C1-H1···O9 = 119.1, H5···O11 = 2.38, C5-H5···O11 = 112.8.

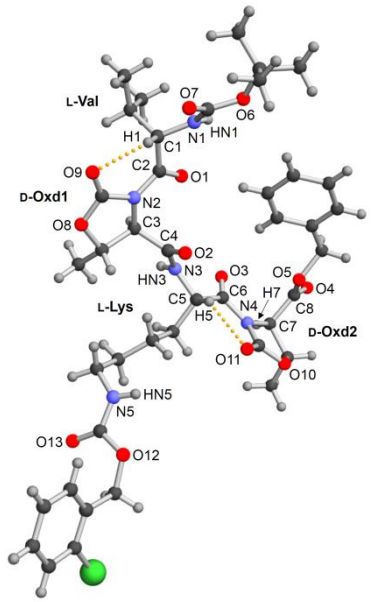

Figure 6. Molecular structure of **3** with atoms drawn as spheres with arbitrary radius. Labelling criteria, H-bond representation and color code are the same as in Figure 5, plus Cl = green. Selected interatomic distances (Å) and angles (°): H1···O9 = 2.28, C1-H1···O9 = 115.0, H5···O11 = 2.32, C5-H5···O11 = 113.5.

Conclusions

Some selected foldamers containing the D-Oxd moiety alternated with a L-amino acid and coupled with Rhodamine B (RB) have been prepared to check their behavior towards purified human lymphocytes, granulocytes, monocytes and HeLa cells. All these molecules show a good biocompatibility, with no detrimental effects up to 64 μM concentration.

The conformational analysis performed in solution and in the solid state suggests that only the longer oligomer of the L-Ala series (**22**) folds into a well-established 3_{10} helix, while the other oligomers give partially unfolded turn structures. A quantitative study was obtained by dose and time response analysis by FACS of human HeLa cells, and primary blood lymphocytes, granulocytes and monocytes incubated with foldamers using H-L-Ala-P-RB as a comparison. Among the analyzed cell types, monocytes and granulocytes associate with these oligomers with best efficacy (6-7 times more effectively than HeLa and lymphocytes). Such a sustained cell captured is still visible after 24 h incubation.

The unfolded foldamers **16**, **18** and **20** display a slower kinetics of cell association than **22**. This outcome could be ascribed to the tendency of **22** to fold into a stable helix, although the presence of several positive charges in **16** and **18** should in principle favor cellular uptake.

Given the different chemical structure of the herein characterized molecules, our new evidence further supports the hypothesis that foldamers with helix-like frameworks can favor the association to inflammatory cells, independent of their charge and chemical nature. These oligomers may thus be regarded as possible targeting agents of small drugs for several reasons: they are intrinsically non-toxic to cells at relatively high doses; moreover, if long enough, they show a peculiar cell targeting preference, being rapidly and more effectively internalized in human blood myeloid cells, like monocytes and granulocytes. Although the biochemical basis for such cell selectivity, especially displayed by long (> 2 units) and neutral oligomers, is still poorly understood, the present formulations or improved analogues may be used to target specific cell types. For example, anti-inflammatory drugs may be coupled to appropriate oligomers and directed more selectively to monocytes/granulocytes. Similar foldamers may be refined and serve as alternative targeting agent also for nanoparticles in nanomedicine.

Experimental Details

Synthesis. Solvents were dried by distillation before use. All reactions were carried out in oven-dried glassware. The melting points of the compounds are uncorrected. High quality infrared spectra (64 scans) were obtained with an ATR-FT-IR Bruker Alpha System spectrometer. All spectra were measured in

solutions at 3 mM concentration in dry CH_2Cl_2 using a 1 mm NaCl cell, or at 1% w/w in dry KBr. All compounds were dried *in vacuo* and all sample preparations were performed in a nitrogen atmosphere. NMR spectra were recorded with a Varian Inova 400 spectrometer at 400 MHz (^{1}H NMR) and at 100 MHz (^{13}C NMR). The measurements were carried out in D_2O or in $CDCl_3$. The proton signals were assigned by *g*COSY spectra. Chemical shifts are reported in δ values relative to the solvent (D_2O or $CDCl_3$) peak. The (4*R*,5*S*)-4-benzoxycarboxy-5-methyl-oxazolidin-2-one (D-Oxd-OBn) was obtained by following the previously reported procedure.[17]

ECD spectra. ECD spectra were recorded at room temperature on a spectropolarimeter. Quartz cuvettes of 0.2 and 1 mm path length were employed. Foldamers were dissolved in water, yielding clear solutions at approximately 3 mM concentration. The spectra were recorded between 180 and 300 nm for the far-UV and near-UV region, with 0.1 nm resolution. 32 scans were accumulated with a scanning speed of 100 nm/min and a time constant of 1 s and the solvent baseline was subtracted from the averaged spectra. Final spectra are presented in molar ellipticity.

X-ray crystallography. Single-crystal X-ray diffraction studies were carried out at 115(2) K on compounds *rac*-Boc-L-Ala-D-Oxd-OBn (from chloroform), Boc-(D-Ala-L-Oxd)$_2$-OBn (from chloroform) and **3** (from ethyl acetate) with a four-circle Bruker X8-APEX diffractometer equipped with a Mo-Kα generator (λ = 0.71073 Å), an area detector and a Kryo-Flex cryostat, and controlled by Bruker-Nonius X8APEX software. The structures were solved and refined on F_o^2 by standard methods using the WINGX v2013.3 package [52] in conjunction with SIR92 [53] and SHELXL-2014/7 [54] programs. Compound *rac*-Boc-L-Ala-D-Oxd-OBn crystallizes in monoclinic space group $P2_1/n$ (Z = 4) whereas crystals of Boc-(D-Ala-L-Oxd)$_2$-OBn and **3** belong to monoclinic space group $P2_1$ (Z = 2). Disorder effects were limited to the 2Cl-Z substituent in **3**, which was refined over two positions with 0.919(2) and 0.081(2) occupancies. The minority component was restrained to have the same geometry as the majority component within 0.01 and 0.02 Å for 1,2- and 1,3-distances, respectively. Furthermore, its NC(O)O and 2-Cl-Ph moieties were restrained to be flat and all minority atoms were refined with a common isotropic displacement (ID) parameter. All remaining nonhydrogen atoms in the structures were refined anisotropically. Hydrogen atoms were treated with ID parameters but only in *rac*-Boc-L-Ala-D-Oxd-OBn they were subject to unrestrained refinement. Amide hydrogens in Boc-(D-Ala-L-Oxd)$_2$-OBn and **3** were refined independently with N-H distances restrained to 0.880(15) Å and a unique ID parameter in **3**. Aromatic, tertiary and methylene hydrogens in Boc-(D-Ala-L-Oxd)$_2$-OBn and **3** were added in idealized positions and allowed to ride on the parent carbon atom, with U(H) = 1.2U_{eq}(C). Methyl hydrogens were also treated as riding contributors but with torsion angle refinement (AFIX 137), and a common ID parameter *per* CH_3 group in Boc-(D-Ala-L-Oxd)$_2$-OBn or U(H) = 1.5U_{eq}(C) in **3**.
Thanks to the chlorine atom in the partially-disordered 2Cl-Z group, the absolute configuration expected for **3** was confirmed by anomalous dispersion effects using Mo-Kα radiation. In the same conditions, the absolute structure of Boc-(D-Ala-L-Oxd)$_2$-OBn could not be established with certainty, but the Flack parameter (x) suggests that the measured crystal is likely to entail D-Ala and L-Oxd residues, as written (x = -1.4(5) vs. 2.4(5) for the inverted model). CCDC 1493119-1493121 contain the supplementary crystallographic data for this paper. These data can be obtained free of charge from the Cambridge Crystallographic Data Centre via www.ccdc.cam.ac.uk/data_request/cif.

Cell isolation and culture. HeLa cells were maintained in DMEM medium (Gibco) supplemented with 10% FCS (Euroclone) and antibiotics (penicillin and streptomycin, Invitrogen) at 37°C in a humidified atmosphere containing 5% (v/v) CO_2; cells were split every 2-3 days.
Human monocytes, granulocytes and lymphocytes were purified from buffy coats of healthy donors, kindly provided by the Centro Immunotrasfusionale, Hospital of Padova. Briefly, for monocytes purification, buffy coats were subjected to two sequential centrifugations on Ficoll and Percoll gradient (GE Healthcare); residual lymphocytes were removed by incubation in 2% FCS RPMI at 37 °C and subsequently removed by washing. Unless otherwise specified, cells were kept at 37 °C in a humidified atmosphere containing 5% (v/v) CO_2 in RPMI-1640 supplemented with 10% FCS. For granulocytes purification, the pellet of cells obtained after the centrifugation on Ficoll gradient was subjected to dextran erythrocyte precipitation; residual erythrocytes were removed by hypotonic lysis in 155 mM NH_4Cl, 10 mM $KHCO_3$, and 100 mM Na_2EDTA at pH 7.4 and cells were cultured in RPMI medium, supplemented with 10% FCS. For lymphocytes preparation, buffy coats were incubated with 50 µl/ml of Rosette Sep® Human T Cell Enrichment Cocktail (StemCell Technologies). Blood was then centrifuged over a Ficoll gradient and cells were cultured in RPMI medium, supplemented with 10% FCS.

MTS cytotoxicity assay. HeLa cells (1 x 10^6 cells/mL) were plated into a 96-well culture plate the day before the experiment. Cells were then incubated for 18 h with different oligomers at different concentrations (up to 50 µM) in DMEM additioned with 10% FCS. Cellular mitochondrial activity (indicator of cellular viability) was evaluated by MTS assay (Promega) according to the instruction manual.

Oligomer association to cells. Intracellular distribution of labelled-oligomers was assessed by confocal microscopy. Human purified monocytes (2x10^5) were seeded on cover glasses and after 24h they were incubated for 18h at 37°C with oligomers, washed with PBS and directly analyzed by confocal microscopy (Leica SP2). Images were processed using ImageJ software. Alternatively, monocytes, granulocytes, lymphocytes or HeLa cells (2x10^5 cells/well) were incubated with labelled-oligomers for 3 or 24 hours at 37°C. Cell MFI (mean fluorescence intensity) values were obtained by cytofluorimetry (FACSCanto, BD) and analyzed by FACSDiva Software (BD).

Keywords: bioconjugates • conformational analysis • foldamers • leukocytes • peptides

[1] R. Wombacher, V. W. Cornish, *J. Biophotonics* **2011**, *4*, 391–402.

[2] M. Beija, C. A. M. Afonso, J. M. G. Martinho, *Chem. Soc. Rev.* **2009**, *38*, 2410.

[3] M. Rad-Malekshahi, L. Lempsink, M. Amidi, W. E. Hennink, E. Mastrobattista, *Bioconjug. Chem.* **2016**, *27*, 3–18.

[4] W. S. Horne, S. H. Gellman, *Acc. Chem. Res.* **2008**, *41*, 1399–408.

[5] S. H. Gellman, *Acc. Chem. Res.* **1998**, *31*, 173–180.

[6] A. D. Bautista, C. J. Craig, E. A. Harker, A. Schepartz, *Curr. Opin. Chem. Biol.* **2007**, *11*, 685–692.

[7] B. Brodsky, G. Thiagarajan, B. Madhan, K. Kar, *Biopolymers* **2008**, *89*, 345–353.

[8] C. Bechara, S. Sagan, *FEBS Lett.* **2013**, *587*, 1693–1702.

[9] S. S. Shankar, S. N. Benke, N. Nagendra, P. L. Srivastava, H. V Thulasiram, H. N. Gopi, *J. Med. Chem.* **2013**, *56*, 8468–8474.

[10] S. Fahs, Y. Patil-sen, T. J. Snape, *Chem.Soc.Rev.* **2015**, *16*, 1840–1853.

[11] C. Tomasini, G. Angelici, N. Castellucci, *European J. Org. Chem.* **2011**, 3648–3669.

[12] S. Lucarini, C. Tomasini, *J. Org. Chem.* **2001**, *66*, 727–732.

[13] N. Zanna, L. Milli, B. Del Secco, C. Tomasini, *Org. Lett.* **2016**, *18*, 1662–1665.

[14] C. Tomasini, V. Trigari, S. Lucarini, F. Bernardi, M. Garavelli, C. Peggion, F. Formaggio, C. Toniolo, *European J. Org. Chem.* **2003**, *4*, 259–267.

[15] C. Tomasini, G. Luppi, M. Monari, *J. Am. Chem. Soc.* **2006**, *128*, 2410–2420.

[16] G. Angelici, G. Luppi, B. Kaptein, Q. B. Broxterman, H. J. Hofmann, C. Tomasini, *European J. Org. Chem.* **2007**, 2713–2721.

[17] G. Luppi, C. Soffrè, C. Tomasini, *Tetrahedron Asymmetry* **2004**, *15*, 1645–1650.

[18] B. P. Mowery, S. E. Lee, D. a. Kissounko, R. F. Epand, R. M. Epand, B. Weisblum, S. S. Stahl, S. H. Gellman, *J. Am. Chem. Soc.* **2007**, *129*, 15474–15476.

[19] I. M. Rio-Echevarria, R. Tavano, V. Causin, E. Papini, F. Mancin, A. Moretto, *J. Am. Chem. Soc.* **2011**, *133*, 8–11.

[20] R. Tavano, G. Malachin, M. De Zotti, C. Peggion, B. Biondi, F. Formaggio, E. Papini, *Biochim. Biophys. Acta - Biomembr.* **2015**, *1848*, 134–144.

[21] M. Sameiro, T. Gonçalves, *Chem. Rev.* **2009**, *109*, 190–212.

[22] N. Agarwal, P. Srivastava, S. K. Raghuwanshi, D. N. Upadhyay, S. Sinha, P. K. Shukla, V. Ji Ram, *Bioorganic Med. Chem.* **2002**, *10*, 869–874.

[23] B. E. Haug, W. Stensen, M. Kalaaji, Ø. Rekdal, J. S. Svendsen, *J. Med. Chem.* **2008**, *51*, 4306–4314.

[24] P. Palladino, D. A. Stetsenko, *Org. Lett.* **2012**, *14*, 6346–6349.

[25] S. Kirkham, I. W. Hamley, A. M. Smith, R. M. Gouveia, C. J. Connon, M. Reza, J. Ruokolainen, *Colloids Surfaces B Biointerfaces* **2016**, *137*, 104–108.

[26] J. Lohse, P. E. Nielsen, N. Harrit, O. Dahl, *Bioconjug. Chem.* **1997**, *8*, 503–9.

[27] T. Nguyen, M. B. Francis, *Org. Lett.* **2003**, *5*, 3245–3248.

[28] L. Belvisi, C. Gennari, A. Mielgo, D. Potenza, C. Scolastico, *European J. Org. Chem.* **1999**, 389–400.

[29] J. Yang, S. H. Gellman, *J. Am. Chem. Soc.* **1998**, *120*, 9090–9091.

[30] B. Imperiali, R. A. Moats, S. L. Fisher, T. J. Prins, *J. Am. Chem. Soc.* **1992**, *114*, 3182–3188.

[31] C. Toniolo, F. Formaggio, R. W. Woody, *Compr. Chiroptical Spectrosc. Vol. 2 Appl. Stereochem. Anal. Synth. Compd. Nat. Prod. Biomol.* **2012**, *2*, 499–543.

[32] C. M. Venkatachalam, *Biochim. Biophys. Acta* **1968**, *168*, 411–416.

[33] C. Toniolo, F. Formaggio, S. Tognon, Q. B. Broxterman, B. Kaptein, R. Huang, V. Setnicka, T. a. Keiderling, I. H. McColl, L. Hecht, et al., *Biopolymers* **2004**, *75*, 32–45.

[34] C. Toniolo, a Polese, F. Formaggio, M. Crisma, J.

Kamphuis, *J. Chem. Soc. Chem. Commun.* **1996**, *118*, 2744–2745.

[35] M. C. Manning, R. W. Woody, *Biopolymers* **1991**, *31*, 569–586.

[36] B. W. Matthews, *Protein Sci.* **2009**, *18*, 1135–1138.

[37] D. E. Hague, J. R. Idle, S. C. Mitchell, R. L. Smith, *Xenobiotica* **2011**, *41*, 837–843.

[38] W. Cai, J. Marciniak, M. Andrzejewski, A. Katrusiak, *J. Phys. Chem. C* **2013**, *117*, 7279–7285.

[39] F. Faigl, E. Fogassy, M. Nògràdi, E. Pàlovics, J. Schindler, *Tetrahedron Asymmetry* **2008**, *19*, 519–536.

[40] M. Pellegrini, S. W. Wukovitz, T. O. Yeates, *Proteins* **1997**, *28*, 515–21.

[41] T. O. Yeates, S. B. H. Kent, *Annu. Rev. Biophys.* **2012**, *41*, 41–61.

[42] P. K. Mandal, G. W. Collie, B. Kauffmann, I. Huc, *Angew. Chem. Int. Ed. Engl.* **2014**, 14424–14427.

[43] B. L. Pentelute, Z. P. Gates, V. Tereshko, J. L. Dashnau, J. M. Vanderkooi, A. A. Kossiakoff, S. B. H. Kent, *J. Am. Chem. Soc.* **2008**, *130*, 9695–9701.

[44] I. Saha, B. Chatterjee, N. Shamala, P. Balaram, *Biopolym. - Pept. Sci. Sect.* **2008**, *90*, 537–543.

[45] R. Fanelli, L. Milli, A. Cornia, A. Moretto, N. Castellucci, N. Zanna, G. Malachin, R. Tavano, C. Tomasini, *European J. Org. Chem.* **2015**, *2015*, 6243–6248.

[46] L. Milli, M. Larocca, M. Tedesco, N. Castellucci, E. Ghibaudi, A. Cornia, M. Calvaresi, F. Zerbetto, C. Tomasini, *J. Org. Chem.* **2014**, *79*, 5958–5969.

[47] G. Luppi, R. Galeazzi, M. Garavelli, C. Tomasini, *Org. Biomol. Chem.* **2004**, *2*, 2181–2187.

[48] G. Angelici, G. Falini, H.-J. Hofmann, D. Huster, M. Monari, C. Tomasini, *Angew. Chemie Int. Ed.* **2008**, *47*, 8075–8078.

[49] G. Angelici, G. Falini, H. J. Hofmann, D. Huster, M. Monari, C. Tomasini, *Chem. - A Eur. J.* **2009**, *15*, 8037–8048.

[50] N. Zanna, L. Milli, B. Del Secco, C. Tomasini, Org. Lett. **2016**, *18*, 1662-1665.

[51] G. Longhi, S. Abbate, F. Lebon, N. Castellucci, P. Sabatino, C. Tomasini, *J. Org. Chem.* **2012**, *77*, 6033–6042.

[52] L. J. Farrugia, *J. Appl. Crystallogr.* **2012**, *45*, 849–854.

[53] A. Altomare, G. Cascarano, C. Giacovazzo, A. Guagliardi, *J. Appl. Crystallogr.* **1993**, *26*, 343–350.

[54] G. M. Sheldrick, *Acta Crystallogr. Sect. C Struct. Chem.* **2015**, *71*, 3–8.

Entry for the Table of Contents

FULL PAPER

Text for Table of Contents

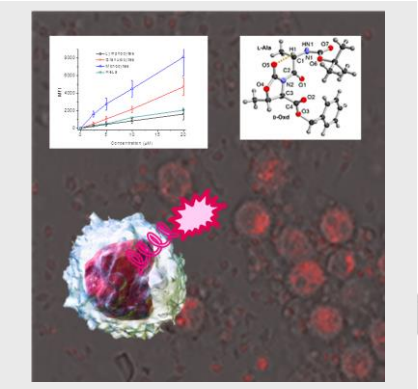

Benedetta Del Secco, Giulia Malachin, Lorenzo Milli, Nicola Zanna, Emanuele Papini, Andrea Cornia, Regina Tavano,* Claudia Tomasini**

Page No. – Page No.

Title